INT. J. REMOTE SENSING, 1998, VOL. 19, NO. 7, 1299–1317

Landsat TM image texture and moisture variations of the soil surface under the rainforest of the Rondônia state, Brazil

F. SEYLER

L'Institut Français de Recherches Scientifiques pour le Développement en Coopération (ORSTOM)

M. BERNOUX and C. C. CERRI

Centro de Energia Nuclear na Agricultura (CENA/USP), CP 96, 13400–970 Piracicaba SP, Brazil

(*Received 31 October 1996; in final form 28 July 1997*)

Abstract. A Landsat TM image, part of a rainforest located in the state of Rondônia, Brazil, was analysed using Fourier transform techniques in order to extract textural features. The lattice-like texture pattern recorded was then compared with the geological structural trends of the area, and measures of the soil surface moisture treated by geostatistical analysis. The consistency between the different sets of analysis suggests that the spatial distribution of moisture at the soil surface is related to the structure of the bedrock. The near infrared channel of the Landsat TM may be used to record trends in water content distributions at the soil surface under homogeneous forest canopies.

1. Introduction

This paper seeks to relate texture features extracted from a Landsat TM image together with moisture analysis of surface soil samples from a forested area in Rondônia, Brazil. It demonstrates how the textural pattern of homogeneous dense forest cover in the near infrared part of the spectrum matches moisture variation co-structure at the soil surface, and that the lattice-like organization of these moisture variations follows geological structural trends.

Increasing research interest in tropical forest ecosystems has induced numerous studies on the visible and near infrared response of the canopies (Leprieur and Baret 1991, Rock *et al.* 1994). Theoretical studies on bidirectional reflectance allow to model this response as a function of viewing-incidence angle, solar-zenithal angle and illumination direction (Deering *et al.* 1994, Jackson *et al.* 1990, Ranson *et al.* 1994), vegetation geometry and water content (Jackson and Pinter 1986, Li and Strahler 1992, Tucker 1980, Moran *et al.* 1989, Penuelas *et al.* 1993). However, these models rarely take into account soil spatial variations and drainage pattern.

It is common to note that soil cannot contribute significantly to bidirectional reflectance of the dense forest canopy (Howard 1991). Nevertheless, geologists are familiar with the interpretation of remote sensing image texture as signature of structural trends or faults, even under a dense forest canopy (Caillon and Borzeix 1992).

Previous research on a rainforest south of Cameroon using remote sensing NIR data showed that a linear textural pattern recorded within homogeneous forest can be related to variations in soil moisture (Riou and Seyler 1995). Experimental studies

0143–1161/98 $12.00

on soil spectral characteristics versus moisture content suggest that differences of moisture in microporosity of the soils might account for the reported NIR luminance variation (Bedidi *et al.* 1992). A method based on Fourier transform has been used to detect the direction and the period of this low-contrasted luminance variation (Riou and Seyler 1997).

The aim of the present study is to compare texture features extracted from a Landsat TM image to moisture analysis of surface soil samples of a forested area in the state of Rondônia.

2. Localization and site characteristics

Our research was conducted in the Nova Vida ranch (10° 09′ S, 62° 48′ W), district of Ariquemes, state of Rondônia (figure 1). The climate in the north of Rondônia is tropical humid, with a short dry season lasting from June to August. The topography is gently undulating in the form of hills, the main type of vegetation being open tropical forest with palms trees. The soil of the ranch (22 000 ha) has been studied by Moraes *et al.* (1996) and classified where the soil samples were realized as red yellow podzolic latosol (EMBRAPA 1988), or as Kandiudult for the U.S. Soil Taxonomy (Soil Survey Staff 1990).

The geological foundation of the area is part of the Xingu complex, that is a crystalline archean basement, formed mainly by gneisses and amphibolites, but also by granulitic and charnockitic rocks. The main faults reported on the geological maps (figure 2(a)) are found in the directions NNE-SSW to NE-SW (N16° E to N55° E), and SE-NW (N130° E to N142° E). The lineations measured for the Xingu complex (figure 2(b)) are, in a decreasing order of importance: N134° E to N150° E; N119° E to N134° E; and N46° E to N60° E.

3. Methodology

3.1. *Remote sensing and image processing*

The study was conducted on a Landsat TM image, path 231, row 67, acquired on 7 July 1991, at the peak of the dry season. The image was obtained from INPE (National Institute for Space Research, Brazil). The channels investigated were channel 3 (TM3 0·63–0·69 μm, red), channel 4 (TM4 0·76–0·90 μm, near infrared), channel 5 (TM5 1·55–1·75 μm, infrared), and channel 7 (2·08–2·35 μm, infrared) at 30 m resolution. The TM4 channel was studied in particular because of its spectral characteristics, which match those of the SPOT XS3 channel used for a previous texture analysis of a rainforest of Cameroon (Riou and Seyler 1995). TM5 and TM7 channels were compared to TM4 channel. First, a spectral analysis was carried out, and four classes of land cover have been chosen: two classes were made within the forest, 'forest 1' which is the darkest part of forest textural component, 'forest 2' which is the brighter one; and two classes were used as reference for the spectral analysis, 'bare soil' and 'old pasture'. The brightness values of these four classes were compared with a simulation of spectral response of standard covers extracted from NASA archives, and calculated with the LOWTRAN 7 model (TeraVue software). The model takes into account the solar-zenithal angle at the date and time of acquisition. The type of atmosphere used for the calculations is the model US62 of LOWTRAN with aerosol repartition of a continental type. The 'visibility' parameter which reflects the atmosphere optical depth has been set at 5 km. The textural analysis was then performed so as to match the field sampling. The area that had been sampled to measure surface soil moisture is shown in figure 1 along with one

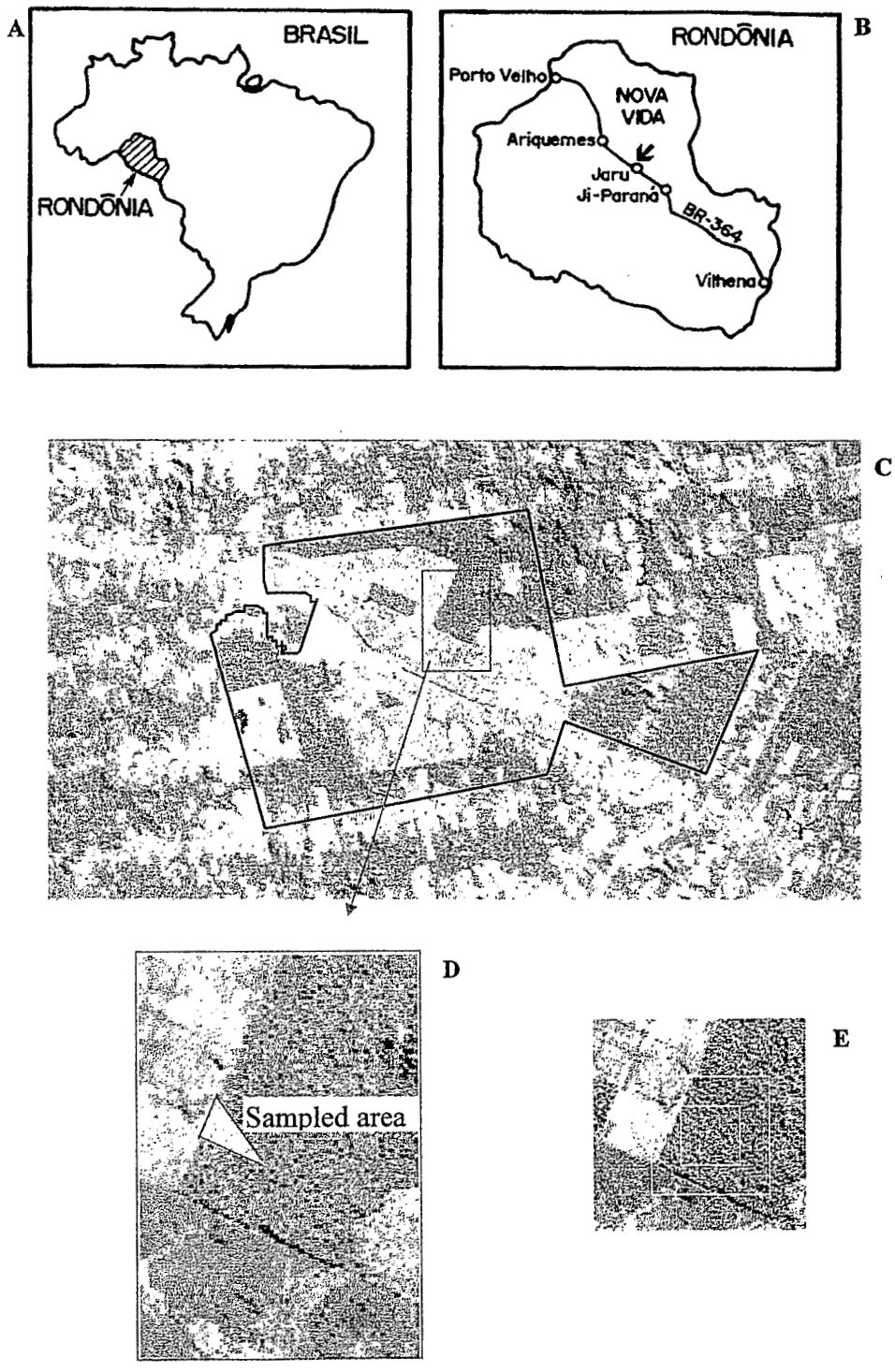

Figure 1. Localization of Nova Vida Ranch in Rondônia State, Brazil (A,B). On Landsat/TM image (path 231, row 67, 7 July 1991), black line represents the Nova Vida ranch boundary (C). Localization on the image of the sampled area, and visualization of two of the windows (64 × 64-pixel and 32 × 32-pixel) used in the image analysis (D). Coloured composite image (Channel 4, 5, 7) realized with PLANET software (ORSTOM).

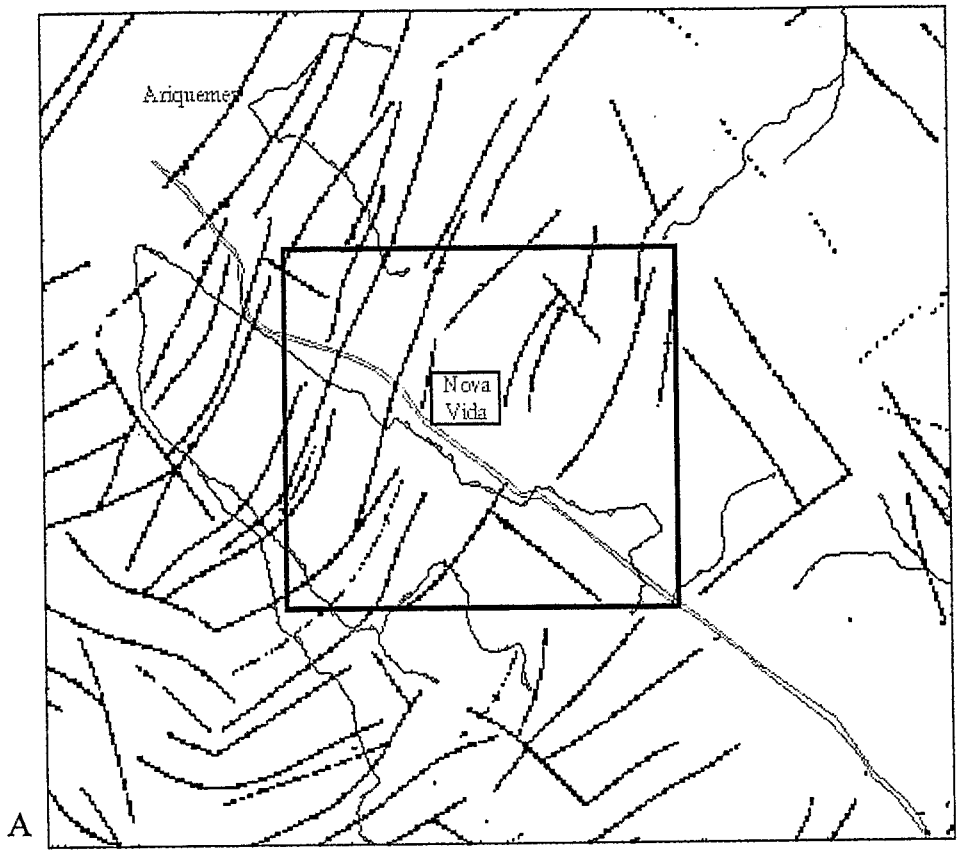

A

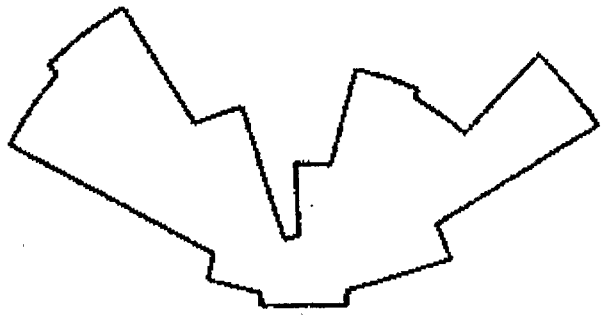

B

Figure 2. Area of Nova Vida ranch extracted from the geological map (Porto Velho, SC 20, RADAMBRASIL, Ministerio das Minas e Energia, 1 : 1 000 000), with the main faults (A). Directions of lineation of Xingu complex (Projeto RADAMBRASIL, levantamento de recursos naturais, Ministerio das Minas e Energia, Vol. 16, p. 116) (B).

of the 64 × 64-pixel and 32 × 32-pixel windows analysed by Fourier transform and frequency filtering. The software used for image processing was PLANET and OSIRIS (ORSTOM). The Fourier transform functions were adapted in order to get rid of frequencies related to edge transitions. Synthetic angular power (SAP) spectrum was reconstructed by rotation of the window and concatenation of the useful parts of two conventional spectra before and after rotation (Riou and Seyler 1997). A moving window of 64 × 64 pixels and a step of 32 pixels in rows and columns allowed us to express graphically the results of the analysis of the spectra obtained for each window. The result is a grid composed of segments whose orientation fits the position of the main frequency peak on the 0–90° or the 90–180° synthetic angular power (SAP) spectrum with an accuracy of 10° (see figure 10).

3.2. *Sample pattern and geostatistical analysis*

At each node on the grids (figure 3), soil samples were collected at a depth of 0–5cm, under natural rainforest, at the end of the dry season (September 1995) and at the end of the rainy season (June 1996). Soil moisture has been determined by weighting soil samples before and after heating at a temperature of 105°. The data treatment were geostatistical, using the theory first presented by Matheron (1965) and first applied to pedometrics by Burgess and Webster (1980 a,b). Geostatistical software used is VARIOWIN.

Semi-variograms of the regionalized variable 'soil moisture' have been estimated by:

$$\gamma^*(h) = (1/2n)\Sigma[Y(j+h) - Y(j)]^2 \quad (1)$$

where $x(j)$ and $x(j+h)$ are the measures of the samples j and $j+h$; h is the distance between two consecutive points of measure; and n is the total number of $(x(j), x(j+h))$ points separated by the distance h.

The spatial structure of surface soil moisture variations was characterized through directional variograms, allowing us to compare the anisotropy of the variable and its range with the angular direction and the period of the image texture obtained by the Fourier analysis. Outlier values (i.e., values more than 1·5 interquartile range [IQR, is the difference between the 75th percentile and the 25th percentile of a variable distribution]) were removed for the geostatistical analysis. Cahn *et al.* (1994)

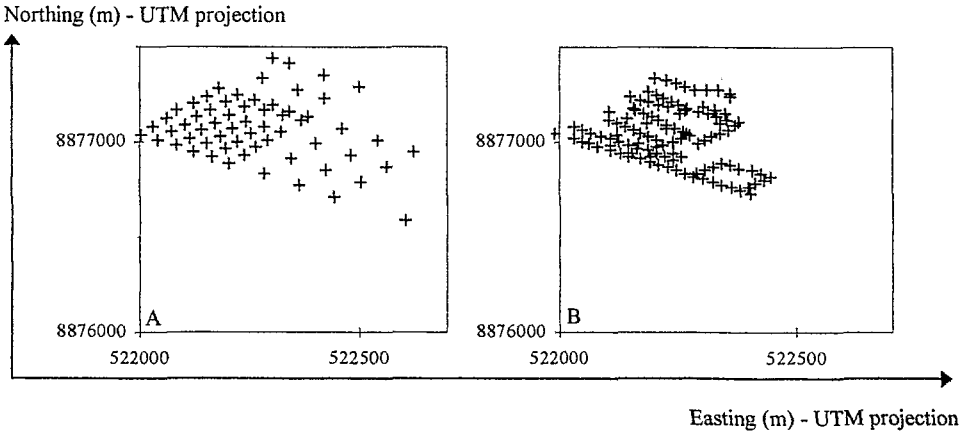

Figure 3. Sample grid used in September 1995 (A) and in June 1996 (B).

suggested that removing outlying data may help in modelling the variance-distance relationship, and Cressie (1993) thought to be sensible deleting outliers when computing a variogram. Outliers are therefore in contradiction with the basic hypothesis of the geostatistical theory, which is the stationary form of the data. In fact, a few outliers were removed: They were only one value for the September 1995 campaign, and two values for the June 1996 campaign (i.e., 0·017 per cent of the sampling) and may very well result in an erratic manipulation or a very peculiar location (very close to a big root, for example).

4. Results and discussion

The texture of the forest, to be further analysed by Fourier transform techniques, comprises low reflectance bands alternating with bands of higher values. In order to make an assumption on how the soil plus the dense forest could be imaged following this texture pattern, each of these two classes of forest reflectance were separated into 'forest 1' and 'forest 2' classes, 'forest 1' being the darker part of the texture. These two classes were then compared with spectral response of standard covers calibrated by the LOWTRAN 7 model. As the visibility parameter was only estimated and not measured, two additional classes, 'bare soil' and 'old pasture' were chosen in order to verify the fitting of the model.

Figure 4 shows the result of the comparison made between the brightness values of the four classes of land cover chosen within the image (forest 1, forest 2, bare soil and old pasture) and the simulated responses. For each class, the average and the standard deviation of the digital values have been calculated for the four bands TM3, TM4, TM5 and TM7. The graph in figure 4 represents with a bold line for each class, the minimum values (min = average-standard deviation) and the maximum values (max = average + standard deviation). The two classes taken as spectral references, 'bare soil' and 'old pasture', are uniform classes (min. and max. values close to each other), and fit quite well to the standard covers whose spectral response were simulated by LOWTRAN7 model. The 'bare soil' class signature is similar to the 'dry soil' signature, especially for the TM4 and TM5 spectral bands. The class 'old pasture' is intermediate between the covers of 'green corn' and 'bean', as could be expected for a pasture which is a mixture of graminaeous (*Bracchiaria brizantha*) and leguminous (*Pueraria sp.*). The matching between the two image classes and the simulated responses shows that the model was well calibrated. The simulated spectral signature, which best matches in terms of shape and value with the class of 'forest 2', is that of 'pine'. Garcia and Alvarez (1994) reported similar patterns of brightness values for a rainforest in a tropical region in southeastern Mexico. For the class 'forest 1', the standard deviation is small for the TM3, TM4 and TM7 bands, and large for the TM5 band. The two classes of forest texture are only separated in the TM4 band. For TM5 and TM7, the brightness values of the 'forest 1' min curve are closer to the 'lake' signature than to the 'pine' signature. In all cases, both shape and value of the curve 'wet soil' were very different from those of the two classes of forest.

These results indicate that the two classes of the forest texture, consisting of alternating bands of dark values and higher ones, cannot be interpreted as spots of bare soil within the canopy, reflecting directly toward the sensor. For the TM4 channel, the class 'forest 1' demonstrates an attenuation of the signal retrieved to the sensor through the forest canopy.

Studies have demonstrated that variations in spectral vegetation indices as the

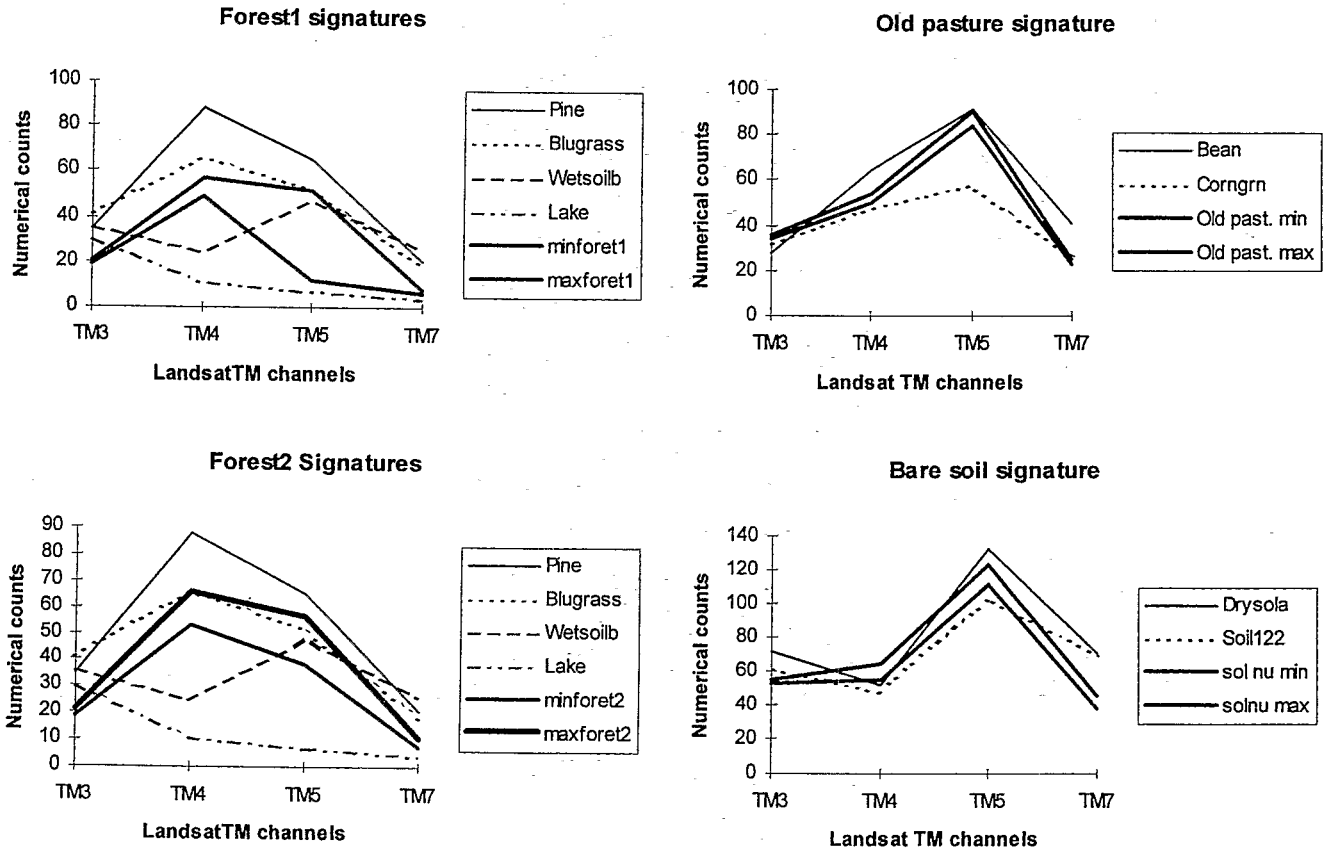

Figure 4. Comparison between the simulated spectral response of standard covers (NASA archives) calculated with LOWTRAN 7 model, and the image numerical counts for 'forest 1', 'forest 2', 'bare soil' and 'old pasture' classes. TeraVue software (Editions de la Boyère).

normalized difference vegetation index (NDVI) for forested areas originate from both canopy optical properties and background spectral reflectance rather than simple variations in leaf area index or percentage canopy closure (Goward *et al.* 1994, Sader *et al.* 1989, Asrar *et al.* 1992). For some authors, soil drainage class and soil texture appear to have a strong effect on NDVI (Levine *et al.* 1994, Lozano Garcia *et al.* 1991). Huete and Jackson (1985) noted the increased influence of soil moisture on the integral brightness of soil-vegetation systems when the vegetation density is above 40 per cent.

Direct measurements of the bidirectional reflectance of forest canopy have been rare, due to the logistical difficulties and the complexity of natural forest stand geometry (Deering *et al.* 1994). Most of them have focused on the effects of changing view angle. Ranson *et al.* (1986), studied the effect of changing forest floor background, measuring bidirectional reflectance of a miniature potted balsam placed on a turntable and variously illuminated. Most of the radiative transfer models (Myneni *et al.* 1992) or geometrical-optical models (Li and Strahler 1986, 1992, Kimes *et al.* 1986) of forest canopies used today do not take into account the diffuse skylight distribution, and the multiple scattered radiations from the ground and crowns. Therefore no definitive assumption can be made about the soil influence on the bidirectional reflectances of forest canopies.

For Brazilian red-yellow latosols, the reflectance variations due to moisture have been extensively studied in the laboratory by Bedidi *et al.* (1992). At 700 nm, the diffuse reflectance of the soil decreases by about 10 per cent when the moisture increases between the air dried sample and the soil at pF 4·2 (which represents the air-entry point into the microporosity, the macroporosity still being free of water). With further increasing moisture, the values of reflectance are oscillating around this value, the lowest one being reached when the soil is at pF 2·8. The high content of iron oxy-hydroxides of these soils enhances the effect of soil moisture on the decrease of the diffuse reflectance.

Riou and Seyler (1995) have demonstrated the role of moisture in the detection of paths under complete canopy closure and therefore undetectable on aerial photographs. On the NIR channel (XS3) of SPOT, the wet sections of these paths are recorded at the end of the rainy season, and they cannot be distinguished from the surrounding forest on the image recorded during the dry season.

The attenuation of the signal retrieved to the sensor through the forest canopy for the TM4 channel could therefore be due to variations in soil moisture between the class 'forest 1'and the class 'forest 2'.

The textural behaviour of the forest (that is, the spatial arrangement between the two classes of texture 'forest 1' and 'forest 2' have then been studied. Figure 5 presents the spectra obtained for the four channels (TM3, TM4, TM5 and TM7) along with the corresponding 64 × 64-pixel windows. The red channel (TM3) and the two infrared channels (TM5 and TM7) have exactly the same textural behaviour, and all of the different spectra that have been analysed have demonstrated an identical texture for these three channels, in spite of their spectral differences. In figure 5, the only structure recorded in these spectral bands is that of the forest-pasture frontier. In some cases, these three channels have recorded a structure other than that of the forest border. For some of the 32 × 32-pixel windows analysed, which do not cover a forest-pasture transition, a structure can be found between N120° E and N160° E (figure 6). In all cases, this structure is weakly expressed (figure 6(b)), the form of the spectra indicates a large and noisy structure in the second quadrant N90° E-

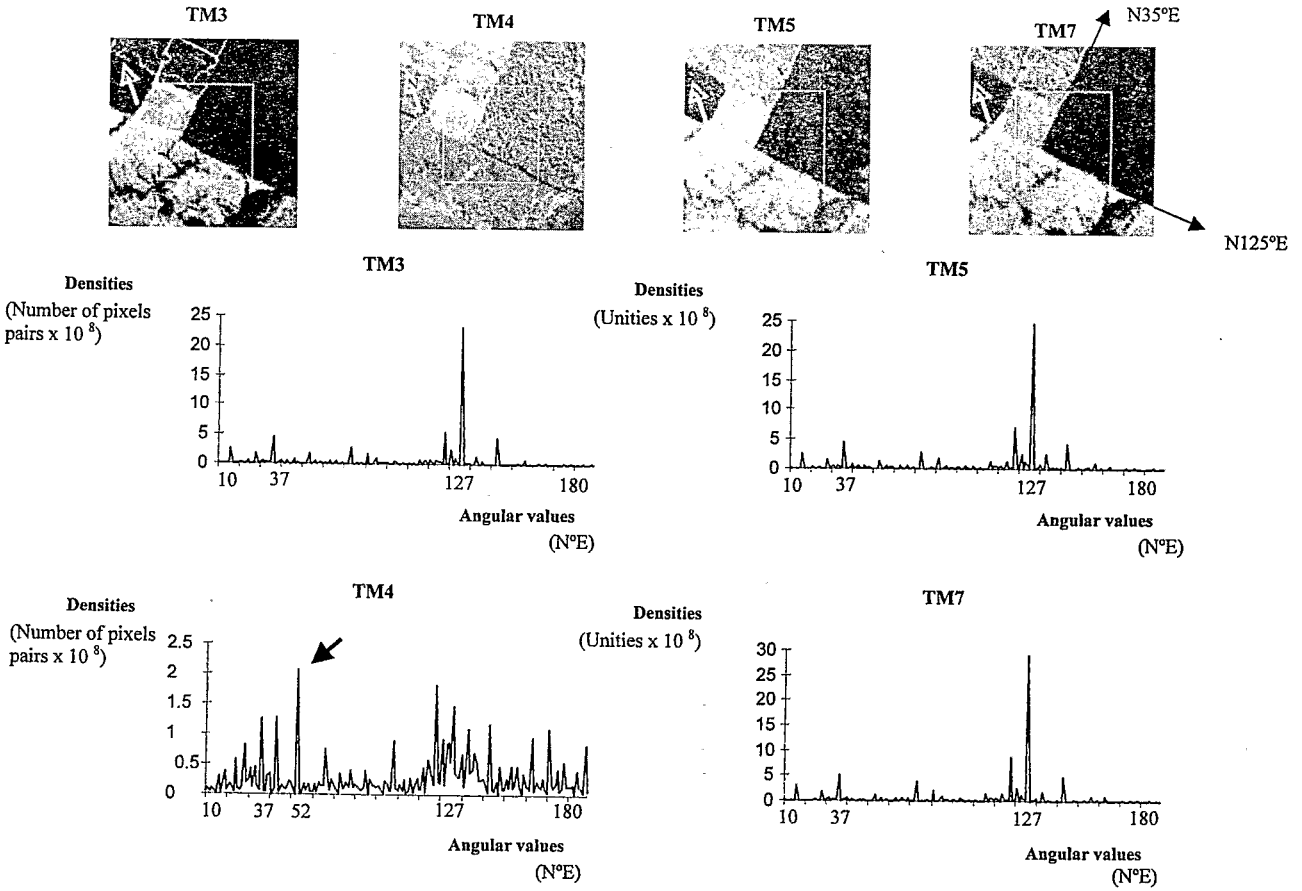

Figure 5. 64 × 64-pixel windows for the four channels (TM3, TM4, TM5, and TM7) along with the corresponding synthetic angular power spectra (64 × 64-pixel windows, filter 3–8 corresponding to a period from 240 to 137 m).

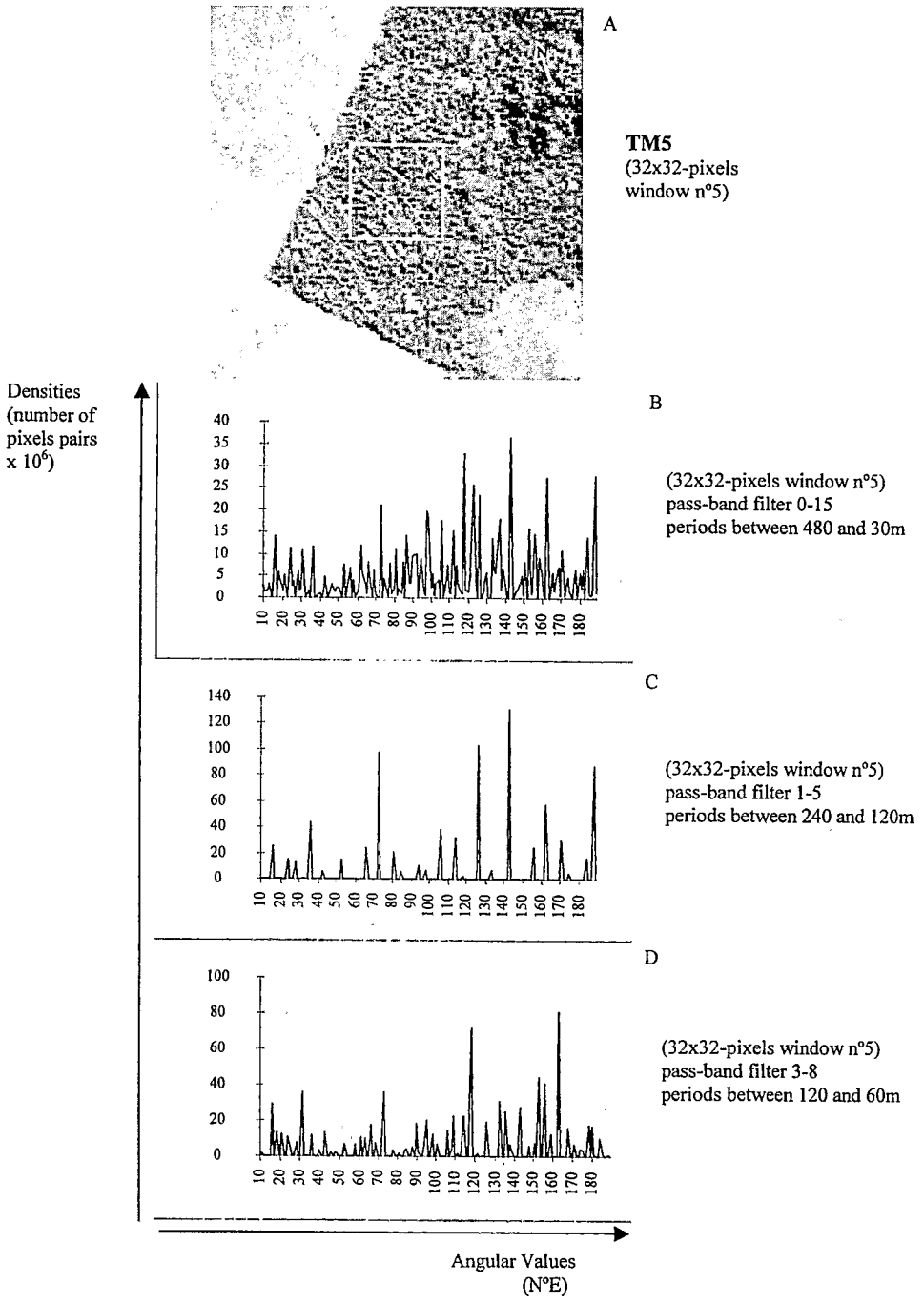

Figure 6. 32 x 32-pixel window extracted from TM5 channel with a forest contrast enhanced (blank lines underline a visible N140° E oriented texture (A), along with the three corresponding spectra with different frequency filtering (B, C and D).

N180° E, and is present all along the frequency spectrum. In figures 6(c) and (d), the structure is present at pass band filter 1–5 which leaves the periods between 240 and 120 m, and at pass-band filter 3–8 which leaves the period between 120 and 60 m.

Figure 5 demonstrates a different behaviour for TM4 channel both in shape and values. The forest-pasture border is also recorded, but with weaker peaks accompanied by close peaks in angular values (between 25 and 42° for the N37° E border and between 118 and 135° for the N127° E border), but the clearer structure (the highest peak) has a direction of N52° E. In figure 7, four 32 × 32 pixel windows extracted from the TM4 channel have been presented along with their respective spectra. Windows 1 and 2 present some structures which can be related with the forest-pasture border. The three windows (2, 3, and 5) which do not match any forest border in the direction N125° E, present structures in the second quadrant (N90° E to N180° E) that are very similar to that observed in the infrared channels (example of the TM5 channel, figure 6). The peaks which are specific to the TM4 channel are signalled by a black arrow. They are enhanced by a frequency filtering centred on the periods from 240 to 120 m. They almost disappear with the frequency filtering centred on the periods between 120 and 60 m. Their direction is remarkably constant at N52° E with another peak varying from the N16° E for window 1 to N38° E for window 3.

We now focus on the results of the geostatistical analysis applied to the water content soil samples. Variance was low (2·87 for the September campaign—dry season, and 4·73 for the June campaign—end of the rainy season). No significant tendency with the hour or day of sampling was found for the two forest data sets. The difference between the lower and the higher value was about 10 per cent of dry soil weight for the two campaigns. The variograms obtained for the two campaigns were remarkably similar to each other (figure 8). Both of them demonstrate a stabilization of the semi-variance for a lag distance between 100 m and 200 m. In figure 9, the maximum and minimum semi-variance are plotted for the two campaigns, in function of the lag distance (m) in abscissa, and the angular direction (trigonometric values) with an accuracy of 15° in ordinate. The curves of minimum and maximum semi-variances for the two campaigns are well separated, indicating a clear anisotropy of the data sets. The curves are close in direction for each campaign, indicating a stability of the structure during the time and seasons. Converting the trigonometric values in N° E values used in the remote sensing study, we find a direction between N40° E and N60° E for the minimum semi-variance and a direction between N140° E and N170° E for the maximum semi-variance values.

The satellite images of the studied area are difficult to obtain because they are covered with clouds during the rainy season, and in bad conditions of nebulosity during the dry season (large occurrence of intensive forest and pasture fires). Furthermore, the remote location of this Amazonian study did not allow us to match the dates between the field campaigns and the remote sensing image. However, the aim of the study was not to retrieve intrinsic values of soil water content, but to compare the structures. Also, the structure obtained for the two soil moisture data sets is remarkably stable during time, although there were chosen to be taken at two contrasted seasons (end of the dry season and end of the rainy season). These two facts allow us to compare this structure with that obtained by remote sensing. Indeed, either the structure is stable during time because it relies mainly on the internal structure of the soil (such as the alteration pattern or the structure of the bedrock), or it is not stable during time because it relies mainly on climatic factors. In the first

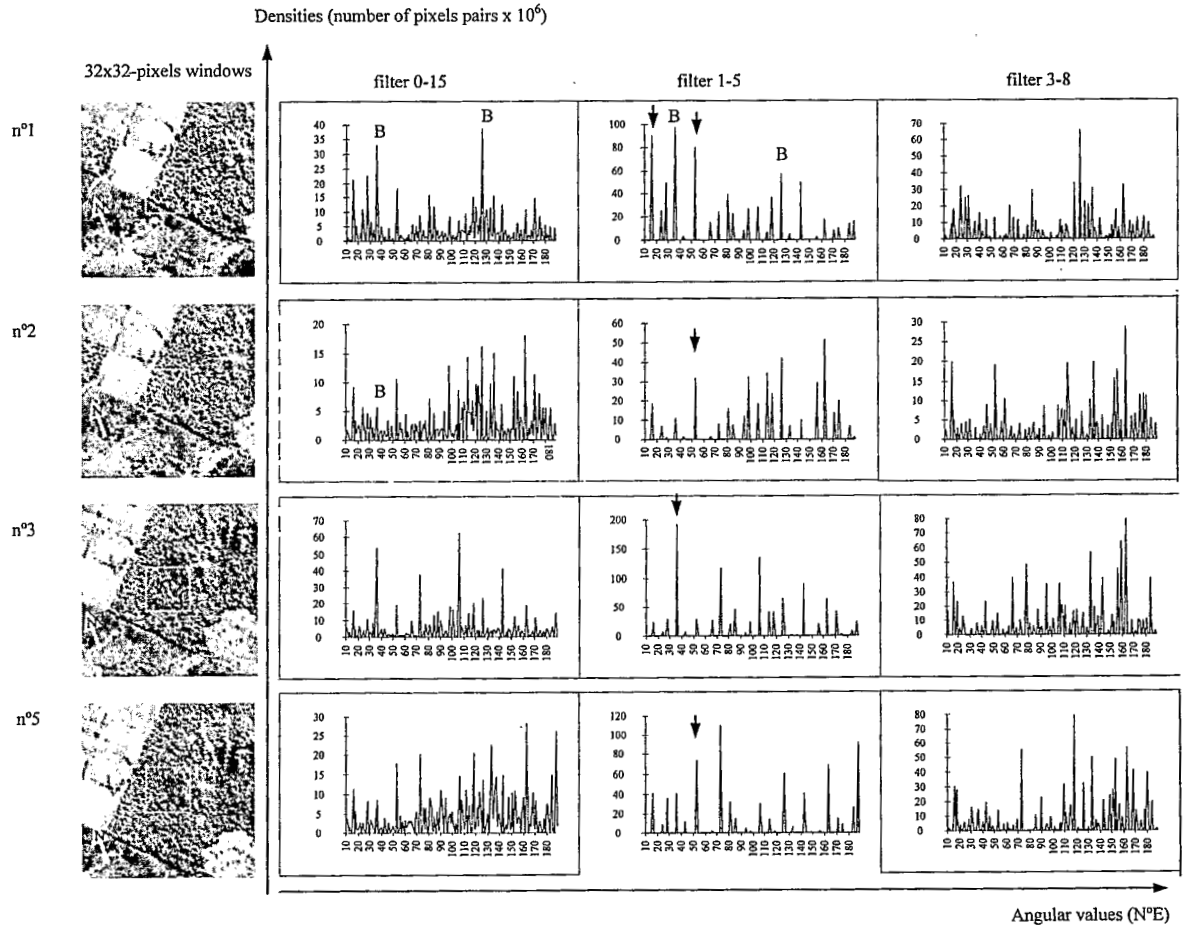

Figure 7. Four 32 × 32-pixel windows extracted from TM4 channel along with their corresponding spectra. The left spectra are calculated with a pass-band filter of 0–15 (corresponding periods between 480 and 30 m), the center spectra are calculated with a pass-band filter of 1–5 (corresponding periods between 240 and 120 m) and the right spectra are calculated with a pass-band filter of 3–8 (corresponding periods between 120 and 60 m). The letter B indicates peaks related to forest-pasture border, and the black arrow signals relevant structure peaks.

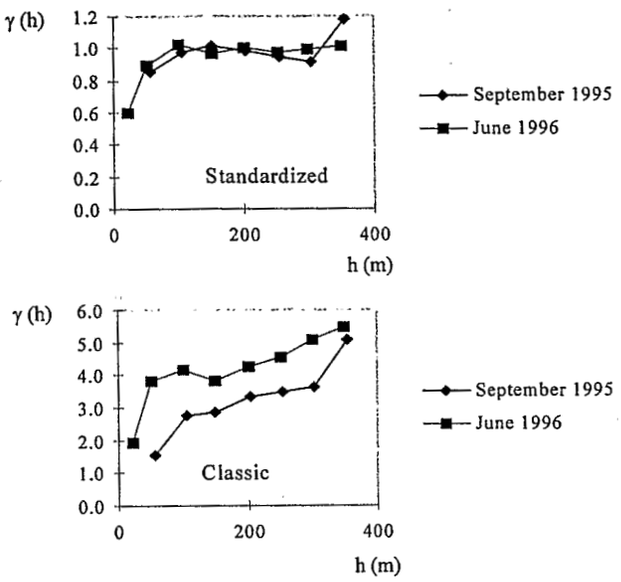

Figure 8. Variograms for the field sampling of September 1995 and June 1996. Variowin software.

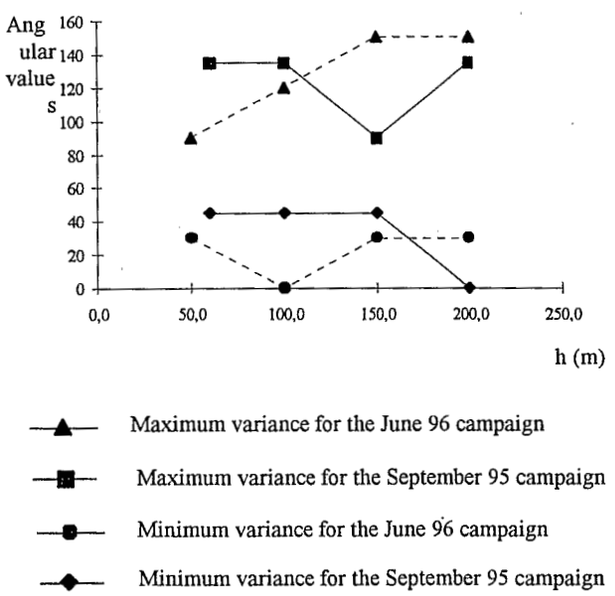

Figure 9. Directional variogram plotting: Maximum and minimum variance for the two data sets in function of the lag distance (h in m) and of the direction (trigonometric values, i.e., the direction 0° in this notation is equivalent to N45° E). Variowin software.

Figure 7. Four 32 × 32 pixel windows extracted from a TM channel using their corresponding spectra. The left spectra are calculated with a pass-band filter of 1–5 pass-band filter of 0–15 (corresponding periods between 480 and 30 m), the center spectra are calculated with a pass-band filter of 3–8 (corresponding periods (corresponding periods between 240 and 120 m) and the right spectra are calculated with a pass-band filter of 3–8 (corresponding periods between 120 and 60 m). The letter B indicates peaks related to forest-pasture border, and the black arrow signals relevant structure peaks.

case, the temporal variation scale would be much more than ten years. In the second case, the variation would be seasonal, or even hourly. The geostatistical study demonstrated that the water content of a single point may vary on an hourly base, but the relative difference in water content between several points at some distance

from each other is stable during time and organized as a structure of hectometric, periodic pattern. Other studies have shown the persistence in time of the spatial structure of soil moisture (Munoz-Pardo *et al.* 1990, Comegna and Basile 1994, McBratney 1992).

When comparing the results of the remote sensing study and the geostatistical study, we can clearly identify the noticeable matching between the period (stabilization of the variance between 100 m and 200 m for the geostatistical analysis—enhancement of the peaks for a frequency filtering corresponding to periods between 240 m and 120 m for the Fourier analysis) and the direction (N40 to 60° E for the geostatistical analysis—N38 to 52° E for the Fourier analysis) of the structure we found.

The measurements of soil surface (0–5cm depth) water content are then organized following a periodic (between 100 m and 200 m) oriented structure. This structure results from a difference of water content of about 10 per cent of dry soil weight (about 10 per cent of water content for minimum values and 20 per cent for maximum values). Studies on the lateritic soils, their structure, porosity and hydrodynamic (Braudeau 1988, Humbel and Pellier 1969, Grimaldi and Boulet 1989), have shown that these soils have a bi-modal porosity, a macroporosity between the aggregates, and a microporosity into the aggregates, that the superficial layers of these soils have a great vertical permeability, and are never saturated with water, even during the rainy season. Bedidi *et al.* (1992) published values of water content for Brazilian latosols: dry lateritic soils—macro and microporosity filled with air—have about 2 per cent to 3 per cent of water content, lateritic soils at the air-entry point in the microporosity have about 20 per cent of water content. The values obtained in this study are intermediate and then suggest that in both cases (minimum and maximum values), the soil is neither dry (i.e., entire microporosity filled with air), nor saturated with water (i.e., macroporosity filled with water). In this water content range (10 per cent to 20 per cent) the difference between samples reside in the respective volume of microporosity voids being filled with water or air. The difference of volume filled with water could be explained by an intrinsic difference of microporosity volume (i.e., textural variation of the soil), or by a sub-soil drainage pattern inferring a differentiated desiccation rate, or both reasons inter-related.

Bedidi *et al.* (1992), working on Brazilian latosols spectral characteristics, showed that, as 'from the dry state until pF 4·2 (air-entry point in the microporosity) only a part of the microporosity is full of water, part of the incident radiation meets a water surface. Since the reflectance of water is very low the total radiation reflected by the soil decreases'. The curves of diffuse reflectance against wavelength published by Bedidi *et al.* (1992: 138), show a maximum difference between air-dried soil and soil at pF 4·2 around a wavelength of 750 nm (near infrared). This, added to the fact that the transmittance of vegetation is maximum for the near infrared part of the spectrum, could be the reason for the seven numerical counts of the TM4 channel which separate the brightest part of the forest texture from the darkest one (mean of 'forest 1' class: 53 ± 4, mean of 'forest 2' class: 60 ± 6).

The matching in both direction and period of the texture measured on the TM4 channel and the spatial structure of water content observed on the field, is reinforcing the assumption that the behaviour of the class 'forest 1' for the TM4 channel could therefore be explained by an attenuation of the signal retrieved towards the sensor by an homogeneous canopy when there is a major absorption by the soil of the transmitted radiation, and not by the direct response of the wet soil (different

response curves; see figure 4). As the spectral behaviour of the TM5 channel is very different from the TM3 and TM7 channels, and their textural behaviour is always the same, it is difficult to infer any relationship between the soil water content organization and the textural behaviour of these channels. In fact, the only structure (except the forest-pasture border) that has been recorded for the channels TM3, TM5 and TM7 has an orientation conform with the maximum semi-variance of the water content samples. But since for these spectral bands, the interaction with the vegetation is much more important than for the TM4 channel, we cannot therefore explain this behaviour.

If we now compare the total of these results with what is known about the geological features of the Nova Vida Farm, it can be identified that the minimum semi-variance of surface water content and the texture of TM4 channel is orientated by following the direction of the main faults (N16° E to N55° E), and that the maximum semi-variance of surface water content and the texture of the four channels (TM3, TM4, TM5 and TM7) is orientated by following the main direction of lineation (N134° E to N150° E). There is a difference in the texture found in one direction as oppose to the other direction. The first one is specifically related to TM4 channel, and it is enhanced by a frequency filtering centred on the period 100 m to 200 m (matching the period obtained for the geostatistical analysis). The second one can be observed independently from the spectral band, and it is multi-frequence. It is also much more 'noisy' (numerous peaks and high amplitude of the adjacent area). This 'coincidence' is worthwhile noting. A relationship made between the direction of main faults and lineation, the 'topographic' pattern of the upper part of the alteritic layer, and the textural and water content distribution pattern of the superficial layer of the soils cannot be excluded, but must be further studied.

This 'coincidence' has been demonstrated for the rainforest of Cameroon (Riou and Seyler 1997). We believe its application for geological survey could be of great importance. For our case study in the area of Nova Vida Ranch, figure 10 presents a subscene of the TM4 channel Landsat scene matching the Nova Vida farm area. The extraction of the direction of the main peak of SAP spectrum for a moving 64 × 64-pixel window has been graphically expressed and superimposed to the image. This figure presents some analogies with figure 2 (geological map), ever though this Rondônia area is not favourable for this type of analysis, because of the forest-pasture patch being very complicated. It is much easier in a homogeneous forest environment, as in the case of rainforest south of Cameroon.

5. Conclusion

Two data sets of surface soil moisture that were sampled at two different period of the year (dry season and end of the rainy season) were analysed by geostatistical techniques and demonstrate a variability pattern constant in space and time. This pattern is periodic, with a period between 100 and 200 meters, and orientated in a direction N40° E to N60° E. This pattern matches a lattice-like texture of Landsat TM4 NIR data analysed by Fourier transform. Both methods are converging towards a model of soil surface variability following a network which period and direction could be predicted by remote sensing images. The consistency between the two sets of analysis and the main geological trends of the area suggests that the spatial distribution of water at the soil surface is organized in relation to the structure of bedrock, even on thick soil layers. These results have several implications.

The fact that near infrared channels of remote sensing satellite are recording

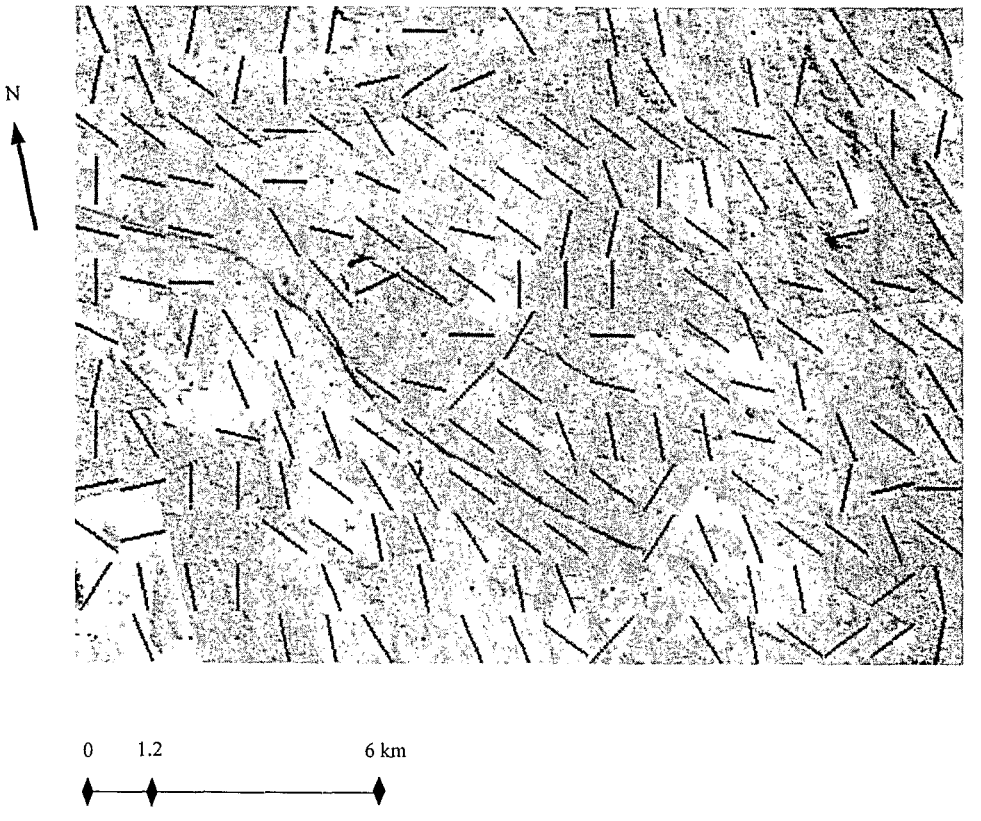

Figure 10. Subscene of the TM4 channel Landsat scene matching the Nova Vida farm area. Superimposed black graphical elements represent the direction (with an accuracy of 10°) of the main peak in the N0–90° E or N90–180° E quadrants (at least five times the average of the ten preceding and the ten following peaks; if no peak reaches this amount, a point figures the lack of significant structure).

these trends in moisture distributions of the soil surface under homogeneous forest canopies is promising for hydrological modelling. The global change models and hydrological models could be greatly improved taking into account the soil parameters, which are nowadays commonly ignored because of the hiatus between soil scientist knowledge and the requirements of mathematical models to deal with quantitative entities. During a NASA workshop on soil moisture (NASA 1995) several scientific issues concerned the spatial and temporal variability. Questions such as 'What spatial-temporal scales of soil moisture are important', or 'Are there any scale-invariant relationships which could be useful in the parameterizations of soil moisture at a range of scales of interest?' were found to be of primarily importance. Charpentier and Grofman (1992), pointed out the importance of the variability patterns of soil moisture in the estimates of trace gas flux, since very little spatial extent of soil, wetter than the mean, can be responsible for the greatest part of the gas flux. Our results show that both questions of spatial scale and invariant relationship could be addressed by NIR texture studies.

This study also demonstrates that geostatistical techniques might be the best way to fill the hiatus between bidirectional reflectance experimental measurements and

image radiometry, achieving the scale step which is the focus of interest of many scientists. It also seems that the combination of geostatistical studies with remote sensing would drastically reduce the cost of soil survey, optimizing the sampling scheme. It would also validate the use of a structure in the outwards of the geostatically studied zone.

Finally, we suggest a better understanding of the relationship between the structural features of the bedrock and the variability pattern of the surface soil layers would be of great import for geological survey.

Acknowledgment

This research was supported by the Centro de Energia Nuclear na Agricultura(CENA), L'Institut Français de Recherches pour le Développement en Coopération(ORSTOM), and by a scholarship and grants from Fundação de Amparo à Pesquisa do Estado de São Paulo(FAPESP). We extend our special thanks to João Arantes Jùnior for access to the site and use of facilities. The authors would like to acknowledge Robert Riou for the stimulation he has given to our research.

References

ASRAR, G., MYNENI, R. B., and CHOUDHURY, B. J., 1992, Spatial heterogeneity in vegetation canopies and remote sensing of absorbed photosynthetically active radiation: a modeling study. *Remote Sensing of Environment*, **41**, 2–3, 85–103.

BEDIDI, A., CERVELLE, B., MADEIRA, J., and POUGET, M., 1992, Moisture effects on visible spectral characteristics of laterite soils. *Soil Science*, **153**, 2, 129–141.

BRAUDEAU, E., 1988, Essai de caractérisation quantitative de l'état structural d'un sol basé sur l'étude de la courbe de retrait. *Comptes Rendus de l' Académie des Sciences*, **T307**, Série II, 1933–1936.

BURGESS, T. M., and WEBSTER, R., 1980 a, Optimal interpolation and isarithmic mapping of soil properties. I. the semi-variogram and punctual kriging. *Journal of Soil Science*, **31**, 315–331.

BURGESS, T. M., and WEBSTER, R., 1980 b, Optimal interpolation and isarithmic mapping of soil properties. II. Block kriging. *Journal of Soil Science*, **31**, 333–341.

CAHN, M. D., HUMMEL, J. W., and BROUER, B. H., 1994, Spatial analysis of soil fertility for site-specific crop management. *Soil Science Society American Journal*, **58**, 1240–1248.

CAILLON, L., and BORZEIX, J., 1992, Reconnaissance à partir des données de SPOT 1 de linéaments géologiques sous couvert végétal dense. Exemple d'application sur des iles volcaniques tropicales. *Photointerprétation*, **5–6**, 233–244.

CHARPENTIER, A., and GROFFMAN, P. M., 1992, Soil moisture variability within remote sensing pixels. *Journal of Geophysical Research*, **97**, D17, 18,987–18,995.

COGMENA, V., and BASILE, A., 1994, Temporal patterns of soil water storage in a cultivated volcanic Vesuvian soil. *Geoderma*, **62**, 299–310.

CRESSIE, N. A. C., 1993, *Statistics for Spatial Data*, Revised Edition, (New York, Wiley).

DEERING, D. W., MIDDELTON, E. M., and ECK, T. F., 1994, Reflectance anisotropy for spruce-hemlock forest canopy. *Remote Sensing of Environment*, **47**, 242–260.

EMBRAPA, 1998, Sistema Brasileiro de classificação de solos, 3rd Approximation, Empresa Brasileira de Pesquisa Agropecuaria, Serviço National de Levantamento e Conservação de solos, (Rio de Janeiro, R.J., Brazil).

GARCIA, M. C., and ALVAREZ, R., 1994, TM digital processing of a tropical forest region in southeastern Mexico. *International Journal of Remote Sensing*, **15**, 8, 1611–1632.

GOWARD, S. N., HUEMMRICH, K. F., and WARING, R. H., 1994, Visible-near infrared spectral reflectance of landscape components in western Oregon. *Remote Sensing of Environment*, **47**, 2, 190–203.

GRIMALDI, M., and BOULET, R., 1990, Relation entre l'espace poral et le fonctionnement hydrodynamique d'une couverture pédologique sur socle de Guyane Française. *Cahiers ORSTOM, Série Pédologie*, **XXV**, 3, 263–277.

HOWARD, J. A., 1991, *Remote Sensing of Forest Resources* (London: Chapman and Hall).

HUETE, A. R., and JACKSON, R. D., 1985, The tasselled cap: size, shape and orientation changes due to soil background. *Machine processing of remotely-sensed data with special emphasis on quantifying global process: models, sensor systems and analytical methods. Proceedings of the 11th Annual Symposium held in West Lafayette, Indiana, on 25–27 June 1985* (West Lafayette, Indiana: Purdue University), pp. 329–337.

HUMBEL, F. X., and PELLIER, J. L., 1969, Porosité, densité et perméabilité de sols ferrallitiques rouge et jaune près de Yaoundé. Office de la Recherche Scientifique et Technique Outre-Mer, (Centre ORSTOM de Yaoundé).

JACKSON, R. D., and PINTER, P. J., 1986, Spectral response of architecturally different wheat canopies. *Remote Sensing of Environment*, **20**, 43–56.

JACKSON, R. D., TEILLET, P. M., SLATER, P. N., FEDOSEJEVS, G., JASINSKI, M. F., HAASE, J. K., and MORAN, M. S., 1990, Bidirectional measurements of surface reflectance for view angle corrections of oblique imagery. *Remote Sensing of Environment*, **32**, 189–202.

KIMES, D. S., NEWCOMB, W. W., NELSON, R. F., and SCHUTT, J. B., 1986, Directional reflectance distributions of a hardwood and a pine forest canopy. *IEEE Transactions on Geosciences and Remote Sensing*, **24**, 281–293.

LEPRIEUR, C. E., and BARET, F., 1991, Modélisation du comportememt d'un couvert végétal dans le M.I.R., apport de la haute résolution spectrale. *Physical measurements and signatures in remote sensing, Proceedings of the 5th International Colloquium held in Courchevel, France, on 4–18 January 1991*, SP-319 (Paris: European Space Agency), pp. 201–204.

LEVINE, E. R., KNOX, R. G., and LAWRENCE, W. T., 1994, Relationship between soil properties and vegetation at the northern experimental forest, Howland, Maine. *Remote Sensing of Environment*, **47**, 2, 231–241.

LI, X., and STRALHER, A. H., 1986, Geometric-optical bidirectional reflectance modeling of a coniferous forest canopy. *IEEE Transactions on Geosciences and Remote Sensing*, **24**, 281–293.

LI, X., and STRALHER, A. H., 1992, Geometric-optical bidirectional reflectance modeling of the discrete crown vegetation canopy: Effect of crown shape and mutual shadowing. *IEEE Transactions on Geosciences and Remote Sensing*, **30**, 276–292.

LOZANO-GARCÍA, D. F., FERNÁNDEZ, R. N., and JOHANNSEN, C., 1991, Assessment of regional biomass-soil relationships using vegetation indexes. *IEEE Transactions on Geosciences and Remote Sensing*, **29**, 331–339.

MAC BRATNEY, A. B., 1992, On variation, uncertainty, and informatics in environmental soil management. *Australian Journal of Soil Research*, **30**, 913–935.

MATHERON, G., 1965, *Les variables régionalisées et leur estimation* (Paris: Masson).

MORAES, J. F. L., VOLKOFF, B., CERRI, C. C., and BERNOUX, M., 1996, Soil properties under Amazon forest and changes due to pasture installation in Rondônia, Brazil. *Geoderma*, **70**, 1, 63–81.

MORAN, M. S., PINTER, P. J., CLOTHIER, B. E., and ALLEN, S. G., 1989, Effect of water stress on the canopy architecture and spectral indices of irrigated alfalfa. *Remote Sensing of Environment*, **29**, 251–261.

MUNOZ-PARDO, J., RUELLE, P., and VAUCLIN, M., 1990, Spatial variability of an agriculture field: geostatistical analysis of soil texture, soil moisture and yield components of two rainfed crops. *Catena*, **17**, 369–381.

MYNENI, R. B., ASRAR, G., and HALL, F. G., 1992, A three-dimensional radiative transfer method for optical remote sensing of vegetated land surfaces. *Remote Sensing of Environment*, **41**, 2–3, 105–121.

NASA, 1995, Soil Moisture. Report of a workshop held in Tiburon, California, 25–27 January 1994, edited by Min-Ying Wei, NASA Conference Publication 3319.

PENUELAS, J., FILELLA, I., BIEL, C., SERRANO, L., and SAVE, R., 1993, The reflectance at the 950–970 nm region as an indicator of plant water status. *International Journal of Remote Sensing*. **14**, 10, 1887–1905.

RANSON, K. J., DAUGHTY, C. S. T., and BIEHL, L. L., 1986, Sun angle, view angle, and background effects on spectral response of simulated balsam fir canopies. *Photogrammetric Engineering and Remote Sensing*, **52,** 649–658.

RANSON, K. J., IRONS, J. R., and WILLIAMS, D. L., 1994, Multispectral bidirectional reflectance of Northern forest canopies with the Advanced Solid State Array Spectroradiometer (ASAS). *Remote Sensing of Environment*, **47,** 276–289.

RIOU, R., and SEYLER, F., 1995, Contribution du sol dans la réflectance proche infrarouge de la forêt tropicale sur images SPOT. *Comptes Rendus de l'Académie des Sciences.* **T320**, série IIa, 1079–1086.

RIOU, R., and SEYLER, F., 1997, Texture analysis of tropical rainforest infrared satellite images: application to structural geology and soil studies. *Photogrammetric Engineering and Remote Sensing*, **63,** 5, 515–521.

ROCK, B. N., WILLIAMS, D. L., MOSS, D. M., LAUTEN, G. N., and KIM, M., 1994, High spectral resolution field and laboratory reflectance measurements of red spruce and eastern hemlock needles and branches. *Remote Sensing of Environment*, **47,** 176–189.

SADER, S. A., WAIDE, R. B., LAWRENCE, W. T., and JOYCE, A. T., 1989, Tropical forest biomass and successional age class relationships to a vegetation index derived from Landsat TM data. *Remote Sensing of Environment*, **28,** 143–156.

SOIL SURVEY STAFF, 1990, Keys to soil taxonomy, 4th ed. SMSS Tech. Monogr., 6.SMSS, Blackburg, Virginia, USA.

TUCKER, C. J., 1980, Remote sensing of leaf moisture in the near infrared. *Remote Sensing of Environment*, **10,** 23–32.